Cyanobenzyl and chlorobenzyl radicals via anion photoelectron imaging spectroscopy

Andrew R. Dixon, Dmitry Khuseynov, Andrei Sanov *

Department of Chemistry and Biochemistry, The University of Arizona, Tucson, AZ 85721, United States

ARTICLE INFO

ABSTRACT

We report the adiabatic electron affinity of the cyanobenzyl radical, EA(PhCHCN) = 1.90 ± 0.01 eV, determined from a combination of the experiment and theory, and assign an upper limit of the EA for the chlorobenzyl radical, EA(PhCHCl) ≤ 1.12 eV. From these results, the C—H bond dissociation energies at the benzyl-α sites of the corresponding closed-shell parent molecules are determined: $80.9 ± 2.3$ kcal mol^{-1} for benzyl nitrile and an upper limit of 84.2 kcal mol^{-1} for benzyl chloride. These results are discussed in terms of substituent interactions and in relation to other similar molecules.

1. Introduction

Organic radicals are important intermediates in a myriad of chemical reactions. Benzyl radicals, in particular, are key players in combustion [1–3]. Their thermodynamic stability and reactivity are greatly affected by the substituent groups. These effects are reflected in the C—H bond dissociation energies (BDE) of the corresponding closed-shell molecules, since the RH → R + H reaction enthalpy is negatively correlated with the stability of the product radical R [4,5].

In this work, we focus on the specific class of doubly substituted methanes, CH$_2$XY, where X and Y are the substituent groups. The electronic structure of these closed-shell molecules is dictated by the nominal sp^3 hybridization of the central carbon atom. This is contrasted by the sp^2 carbon-atom hybridization of the resulting radical, CHXY, in which the unpaired electron is of predominant p character. These electronic-structural properties result in significantly different substituent interactions in the closed-shell parent and the radical.

In general, both π-accepting and π-donating substituent groups tend to stabilize radicals [4]. In a molecular-orbital picture, the stabilization by the π-accepting cyano and unsaturated hydrocarbon groups is due to interaction of the unpaired electron on the radical carbon center with the unoccupied π orbitals of the substituent. In the case of π-donating halogens (F, Cl, Br), the stabilization results from the interaction of the radical-center orbitals with the non-bonding electron pairs of the substituents [3]. In homogenously

substituted radicals with several substituent groups of the same type, substitutions beyond the first tend to have diminishing effects on the radical stability and, therefore, the BDE of the corresponding closed-shell molecule. In the extreme case of fluorine substituents, the radicals are actually destabilized beyond the first substitution [6]. However, when the substitution is heterogeneous, combining π-accepting and π-donating groups, a small synergistic stabilization of the radical is sometimes observed [4,7]. For example, the low C—H BDE values of CH$_2$ClCN and CH$_2$FCN indicate small increases in the respective radical stabilities, compared to the sum of the effects in the corresponding mono-substituted cases [8,9]. This was identified as a captodative effect [7].

While many mono-substituted methyl radicals have been studied, including the benzyl radical CH$_2$Ph [10], where Ph is the phenyl group (C$_6$H$_5$), there is still much to be understood about the effects of multiple heterogeneous substitutions. In this work, we present an anion photoelectron imaging study of the cyanobenzyl (cyanophenylmethyl) and chlorobenzyl (chlorophenylmethyl) radicals. The CN and Cl substituents are well-understood π-accepting and π-donating groups, respectively. Using experimentally measured properties of the radicals and their anions, we indirectly determine the BDEs of the corresponding close-shell molecules, benzyl nitrile and benzyl chloride. The results are discussed in the context of previous investigations of the related homogenously and heterogeneously substituted radicals.

2. Experimental and theoretical methods

The experiments were performed using a custom-built anion photoelectron velocity-map imaging spectrometer, described in detail elsewhere [11,12]. The benzyl nitrile or benzyl chloride

* Corresponding author.
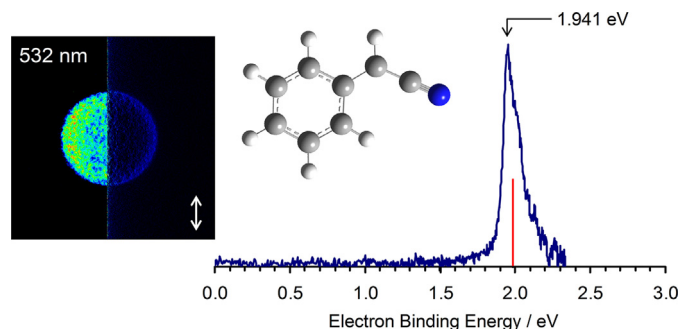E-mail address: sanov@u.arizona.edu (A. Sanov).
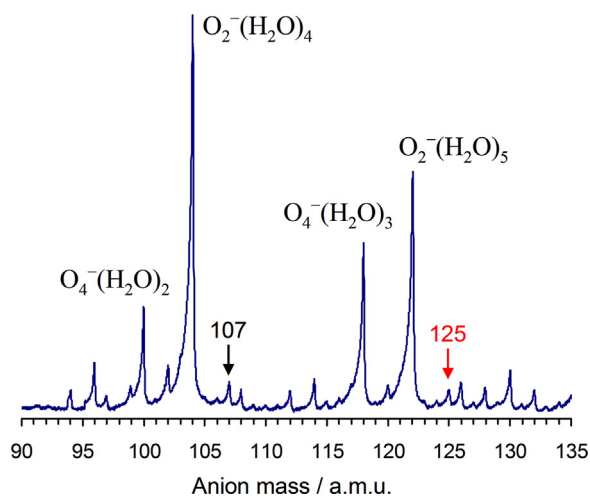
Figure 1. A representative anion mass-spectrum recorded using the benzyl chloride precursor seeded in oxygen, with water impurities present in the gas delivery lines. The anion of interest, PhCHCl⁻, corresponds to the 125 a.m.u. peak, marked with a red arrow. Other ions of the same mass may include the monohydrated methoxyphenide cluster anion, $C_7H_7O^-\cdot H_2O$. The 107 a.m.u. peak, marked with a black arrow, is plausibly assigned to unsolvated $C_7H_7O^-$. (For interpretation of the references to color in this figure legend, the reader is referred to the web version of this article.)

Figure 2. Photoelectron image and corresponding spectrum of the cyanobenzyl anion, PhCHCN⁻, at 532 nm. The double sided arrow indicates the direction of the laser polarization. The red vertical line in the spectrum indicates the VDE value determined from the B3LYP/aug-cc-pVQZ calculations. (For interpretation of the references to color in this figure legend, the reader is referred to the web version of this article.)

precursor was brought into the gas phase by flowing carrier gas, either O_2 or N_2O, over a liquid sample at room temperature. The resulting gas mixture was introduced to the high-vacuum ion-source chamber through a pulsed supersonic nozzle (General Valve Series 9) operated at 20 or 50 Hz to match the laser system used. The supersonic expansion was crossed with a continuous 1 keV electron beam. The O^- ions were formed by dissociative attachment of slow secondary electrons to the carrier gas, while the anions of interest were formed through the well-known deprotonation reactions of O^- with the precursor molecules [13]. The anions were pulse-extracted into a Wiley-McLaren time-of-flight mass spectrometer and detected using a dual microchannel-plate detector with a metal anode. A representative anion mass-spectrum obtained in one of the experiments described in this Letter, specifically for the benzyl chloride precursor seeded in oxygen, is presented in Figure 1. As expected, the mass-spectrum is dominated by hydrated oxygen cluster anions. The anion of interest, PhCHCl⁻ (to be discussed in Section 3.2), corresponds to the 125 a.m.u. peak marked with a red arrow.

The mass-selected anions were interrogated by linearly polarized laser pulses, timed to interact only with ions of a specific mass. Photoelectrons were velocity-mapped [14] in the direction perpendicular to the ion and laser beams and projected onto a 40 mm diameter dual microchannel-plate detector, coupled to a P43 phosphor screen. Photoelectron positions were recorded by a thermoelectrically cooled charge-coupled-device camera. Images were typically accumulated for $\sim 10^6$ experimental cycles. The complete three-dimensional photoelectron distribution was reconstructed via an inverse Abel transformation [15] implemented in the BASEX program [16]. The resulting radial distributions were converted into the electron kinetic energy (eKE) domain using the appropriate Jacobian transformation. The photoelectron spectra were plotted versus electron binding energy (eBE), defined as $eBE \equiv h\nu - eKE$, where $h\nu$ is the photon energy. The spectra were calibrated using the well-known photodetachment transitions of O^- [17,18].

Two laser systems were used in this work. A Spectra-Physics LAB-130 Nd:YAG laser operating at 50 Hz was used to produce

1064 and 532 nm laser light as the fundamental output (5 mJ/pulse) and the second harmonic (3 mJ/pulse) respectively. The 612 nm (10 mJ/pulse) light was produced as the fundamental output of a Continuum ND6000 dye laser running Rhodamine 590 dye and pumped by the second harmonic (532 nm) of a Continuum Surelite II (20 Hz) Nd:YAG laser.

Electronic structure calculations and geometry optimizations were performed using the GAUSSIAN 09 software package [19]. Adiabatic electron affinities (EA) were calculated as the difference in the electronic energy for the anion and neutral species at their respective fully optimized geometries. Vertical detachment energies (VDE) were calculated as the difference in electronic energy for the anion and neutral species, both at the optimized geometry of the anion.

3. Results and analysis

3.1. Cyanobenzyl radical

The photoelectron imaging results for deprotonated benzyl nitrile, i.e. the PhCHCN⁻ anion (116 a.m.u.), are presented in Figure 2. A single band with an onset at about 1.9 eV is observed in the 532 nm image and the corresponding photoelectron spectrum. The maximum position at $eBE = 1.941 \pm 0.003$ eV (determined from the average of several independent runs) is assigned as the VDE of PhCHCN⁻. The slightly negative anisotropy observed in the image is consistent with detachment from the canonical π ($2p$) orbital centered on the radical carbon center.

Geometry optimization and electronic structure calculations using the B3LYP density-functional theory method and a variety of basis sets were carried out for the PhCHCN⁻ anion and the corresponding neutral radical in the respective ground electronic states. From these calculations, the adiabatic EA of PhCHCN and the VDE of the anion were determined and summarized in Table 1.

Table 1
The adiabatic electron affinity (EA) of cyanobenzyl radical and the vertical detachment energy (VDE) of PhCHCN⁻ calculated at the B3LYP level of theory (in eV)[a].

Basis set	EA	VDE	ΔE_{rel}[b]
aug-cc-pVDZ	1.954	1.991	0.036
aug-cc-pVTZ	1.948	1.985	0.037
aug-cc-pVQZ	1.950	1.988	0.038
Experiment	1.90(1)[c]	1.941(3)	–

[a] Values are calculated from electronic energy only.
[b] Defined as $\Delta E_{rel} = VDE_{calc} - EA_{calc}$.
[c] Estimated value, calculated as $EA_{est} = VDE_{exp} - \Delta E_{rel}$. See the text for details.
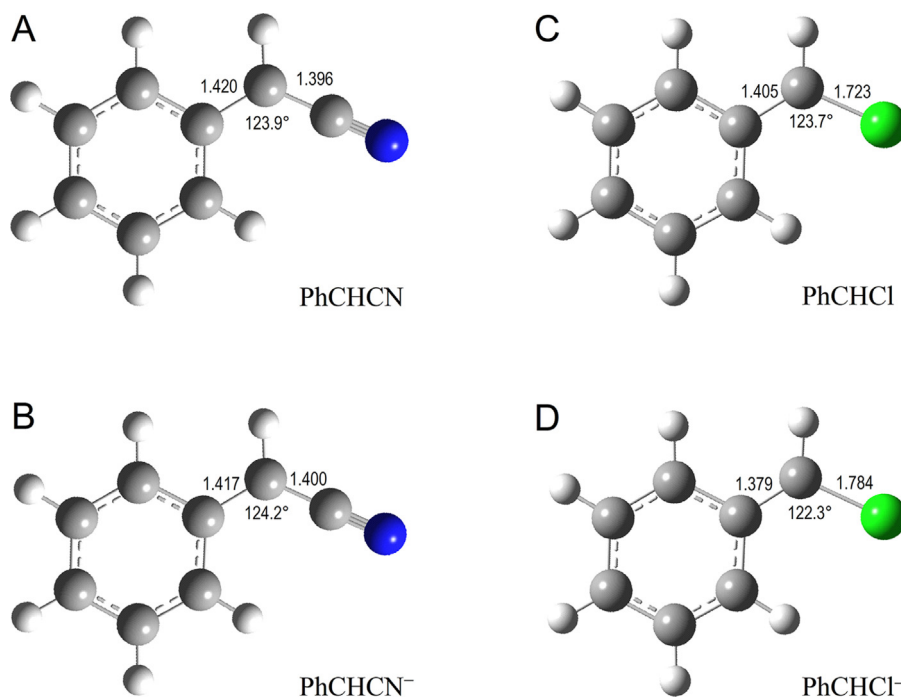
Figure 3. The optimized geometries of (A) the cyanobenzyl radical, (B) the cyanobenzyl anion, (C) the chlorobenzyl radical, and (D) the chlorobenzyl anion. The geometries were optimized at the B3LYP level of theory. Calculations on cyanobenzyl employed the aug-cc-pVQZ basis set, while the chlorobenzyl calculations used the aug-cc-pVTZ basis. Only the key structural parameters are indicated in the figure (bond lengths in – Angstroms, bond angles – in degrees). The complete geometries are provided in Supplementary Content.

The VDE = 1.988 eV, corresponding to the largest basis set used in this study (aug-cc-pVQZ), is also indicated as a red vertical bar in the experimental spectrum in Figure 2. The calculated properties are in good agreement with the experimental results.

The neutral radical and anion geometries optimized with the aug-cc-pVQZ basis are presented in Figure 3(A and B). Only the key structural parameters are indicated in the figure, while the complete geometries are provided in Supplementary Content. The neutral radical is strictly planar, while the anion has a minor (0.07°) out-of-plane puckering of the cyano group indicated by the calculations. Since the energetic barrier at the strict planarity, associated with this distortion, is orders of magnitude smaller than the zero-point vibrational energy, we view this quasi-planar anion structure as effectively planar. Beyond this, there exist only minor differences in the key bond lengths and angles. The very similar anion and neutral geometries, as well as the small difference between the calculated VDE and EA values (Table 1) are consistent with the relatively narrow band observed in the photodetachment (Figure 2).

The EA of cyanobenzyl radical cannot be determined unambiguously directly from the vibrationally unresolved spectrum in Figure 2. However, it can be estimated from the experimental VDE and the theoretically determined relaxation energy of the neutral radical from the anion geometry to the equilibrium structure, ΔE_{rel}. Since ΔE_{rel} equals the difference between the VDE and EA, the EA can be estimated using the relationship: $EA_{est} = VDE_{exp} - \Delta E_{rel}$. In the absence of a direct experimental value, this approach is more advantageous than direct calculation of the EA, because it uses theory only to estimate the relatively small correction from the experimental VDE value (VDE_{exp}). Using $VDE_{exp} = 1.941 \pm 0.003$ eV (Figure 2) and $\Delta E_{rel} = 0.038$ eV (the B3LYP/aug-cc-pVQZ result in Table 1), we estimate EA(PhCHCN) = 1.90 ± 0.01 eV. The uncertainty reflects the range of relaxation energies from different calculations. This EA value agrees well with the approximate band origin in the experimental spectrum in Figure 2.

3.2. Chlorobenzyl radical

The photoelectron imaging results for the low-abundance 125 a.m.u. anion (the mass of PhCHCl⁻) are presented in Figure 4. At 1064 nm only a weak, low-eKE signal is observed (Figure 4A). The spectral feature rises above the noise level at eBE ≈ 1.1 eV. Two partially overlapping features (a) and (b) are apparent in the 612 nm image and the corresponding spectrum (Figure 4B). Modeling the spectrum with a sum of two Gaussians indicates that bands (a) and (b) are centered at eBE = 1.20 and 1.43 eV, respectively, with (a) being significantly narrower than (b).

The geometries of the neutral chlorobenzyl radical and its anion, optimized at the B3LYP/aug-cc-pVTZ level, are shown in Figure 3(C and D), with a complete summary of the structural parameters is given in Supplementary Content. Similar to cyanobenzyl, the equilibrium geometry change expected in the photodetachment of PhCHCl⁻ is small. Again, the neutral is strictly planar, while the anion is effectively planar, with the out-of-plane puckering even smaller than in the cyanobenzyl anion. We do note, however, the 0.03 Å lengthening of the C—Ph bond and the 0.06 Å shortening of the C—Cl bond expected upon the detachment of PhCHCl⁻. Based on these similar geometries, we expect a relatively sharp

Table 2
The adiabatic electron affinity (EA) of the chlorobenzyl radical and the vertical detachment energy (VDE) of PhCHCl⁻ calculated at the B3LYP level of theory (in eV)[a].

Basis set	EA	VDE	ΔE_{rel}[b]
6-311++G**	1.107	1.204	0.097
aug-cc-pVDZ	1.120	1.212	0.092
aug-cc-pVTZ	1.110	1.201	0.091
Experiment	≤1.12	1.20(2)	–

[a] Values are calculated from electronic energy only.
[b] Defined as $\Delta E_{rel} = VDE_{calc} - EA_{calc}$.
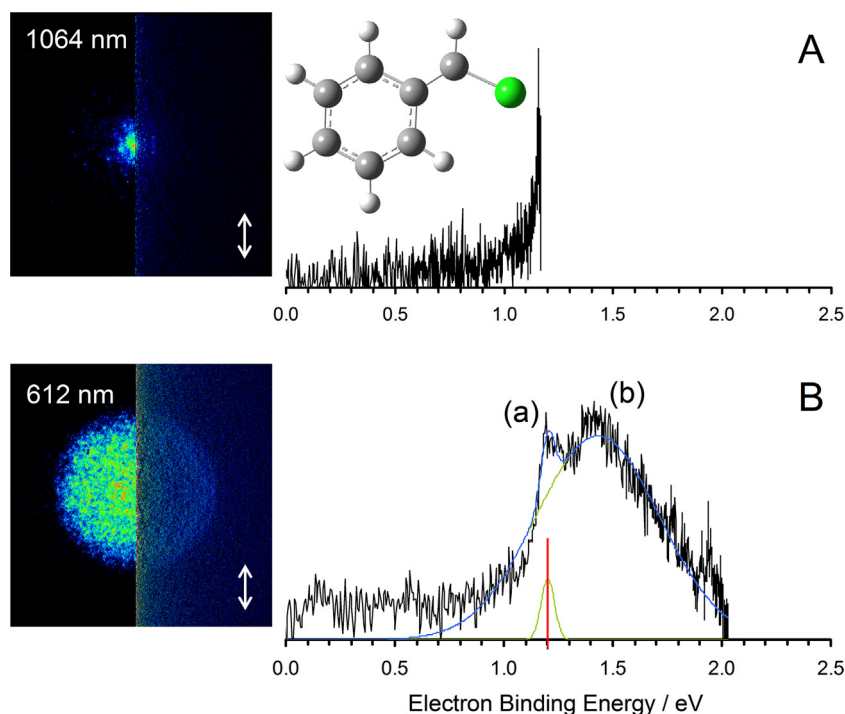
Figure 4. Photoelectron images and corresponding spectra of the 125 a.m.u. anions, obtained at (A) 1064 nm and (B) 612 nm. The double sided arrow indicates the direction of the laser polarization. All signal in (A) and band (a) in (B) are assigned to the chlorobenzyl anion, PhCHCl⁻, while band (b) in (B) corresponds to a different anion of the same mass, plausibly the monohydrated methoxyphenide anion, $C_7H_7O^-\cdot H_2O$. The VDE of PhCHCl⁻, calculated at the B3LYP/aug-cc-pVTZ level of theory, is indicated in (B) with a vertical red line. A global spectral fit with a sum of two Gaussian functions in (B) is shown as a blue curve. The individual Gaussian components (a) and (b) are shown as light-green curves. (For interpretation of the references to color in this figure legend, the reader is referred to the web version of this article.)

PhCHCl⁻ photodetachment feature, qualitatively similar to that observed for PhCHCN⁻ in Figure 2.

The EA values calculated for PhCHCl using three different basis sets (Table 2) agree well with the onset of the transition observed in the low eKE regime at 1064 nm (Figure 4A), as well as with the low-energy wing of band (a) in the 612 nm spectrum (Figure 4B). The VDE values calculated for the anion agree well with the maximum position for band (a). The B3LYP/aug-cc-pVTZ VDE value, 1.201 eV, is indicated in the spectrum with a vertical red line, which agrees essentially perfectly with the peak position of the corresponding Gaussian fit at 1.20 ± 0.02 eV. Therefore, we assign feature (a) to the detachment from PhCHCl⁻. Transition (b), which does not fit any of the predicted properties of PhCHCl⁻, is attributed to the photodetachment of a different anion of the same mass. Calculations at the B3LYP/aug-cc-pVTZ level of theory of the phenide anions and respective neutrals of α-chlorotoulene, deprotonated at the ortho-, meta-, and para- positions, indicated clearly they were not responsible for band (b).

To understand the origin of band (b) in Figure 4B, we turn to the parent-ion mass-spectrum shown in Figure 1. The spectrum is quite congested in the 120–130 a.m.u. region and several alternative ions can account for mass 125 a.m.u., besides PhCHCl⁻. With the abundance of water clusters in the spectrum and the presence of oxygen anions in the ion source, another plausible assignment for the 125 a.m.u. peak in Figure 1 is the cluster of the methoxyphenide anion (deprotonated methoxybenzene, also known as anisole) with water, $C_7H_7O^-\cdot H_2O$. This hypothesis is supported by two observations.

First, a 107 a.m.u. peak, plausibly assigned to $C_7H_7O^-$, is also observed in Figure 1. The 107 and 125 a.m.u. peaks are both marked in the figure with arrows. The two peaks are of comparable intensity, consistent with a sizable $C_7H_7O^-\cdot H_2O$ contribution at 125 a.m.u. Second, the electron affinity of the methoxyphenyl radical has been previously determined through the acidity of

methoxybenzene as EA(C_7H_7O) = 1.12 ± 0.19 eV and 1.25 ± 0.19 eV for the *meta*- and *ortho*-isomers, respectively [20,21]. Accounting for additional stabilization by hydration, band (b) in Figure 4B is consistent with the photodetachment of $C_7H_7O^-\cdot H_2O$.

The above assignment band (b) in Figure 4B to the photodetachment of $C_7H_7O^-\cdot H_2O$ is admittedly not very robust, but the methoxyphenide anion or its clusters are not the focus of this work. The presented hypothesis merely gives a plausible explanation for the additional band in the photodetachment of 125 a.m.u. anions that is not consistent with the predicted properties of the target anion, PhCHCl⁻. Thus, from here on, we focus only on the properties of band (a).

Similar to the cyanobenzyl case, the EA of chlorobenzyl radical cannot be determined unambiguously directly from the vibrationally unresolved data in Figure 4. Due to the overlap of spectral features, the VDE is also subject to scrutiny. Therefore, we can safely assign only an upper bound of the EA, as the eBE value where the spectral feature observed at 1064 nm rises sharply above the noise level, i.e. EA(PhCHCl) ≤ 1.12 eV.

4. The C–H bond dissociation energies of benzyl nitrile and benzyl chloride

From the known EA of the product radical, the corresponding C–H bond dissociation energy of the parent closed-shell molecule can be determined through the general gas-phase acidity/electron affinity thermodynamic cycle [5]:

$$DH_{298}(R-H) = \Delta_{acid}H_{298}(RH) + EA(R) - IE(H)$$

$$+ [\text{thermalcorrections}], \qquad (1)$$

Per this equation, the BDE of the close-shell molecule RH, formally defined as $DH_{298}(R-H)$, is equal to the corresponding enthalpy of deprotonation (acidity), $\Delta_{acid}H_{298}(RH)$, plus the electron affinity

Table 3
Bond dissociation energies of select substituted methanes (in kcal mol^{-1}).

Compound	DH_{298}	Reference	RSE[a]
CH$_4$	104.9 ± 0.4	[5]	0
Phenyl-methanes			
CH$_3$Ph	89.8 ± 0.5	[10]	15.1 ± 0.6
CH$_2$Ph$_2$	81.3 ± 3.1[b]	[21,25]	23.6 ± 3.1
Chloro-methanes			
CH$_3$Cl	100.1 ± 0.6	[6]	4.8 ± 0.7
CH$_2$Cl$_2$	95.7 ± 0.5	[6]	9.2 ± 0.6
CHCl$_3$	93.8 ± 0.6	[6]	11.1 ± 0.7
Cyano-methanes			
CH$_3$CN	94.2 ± 2.0	[26,27]	10.7 ± 2.0
CH$_2$(CN)$_2$	88.7 ± 2.1	[8,27]	16.2 ± 2.1
Benzyl nitrile (cyanophenylmethane)			
PhCH$_2$CN	80.9 ± 2.3[c]	This work	24.0 ± 2.3[c]
Benzyl chloride (chlorophenylmethane)			
PhCH$_2$Cl	≤84.2	This work	≤20.7

[a] Radical (R) stabilization energy, defined as RSE = DH_{298}(CH$_3$—H) − DH_{298}(R—H).
[b] Value calculated with EA and $\Delta_{acid}H_{298}$ from Refs. [21,25] using Eq. (1).
[c] Value and error estimated from experimental and theoretical results, see the text for details.

of the radical, EA(R), minus the ionization energy of the hydrogen atom, IE(H) = 13.60 eV. The thermal corrections contributing to Eq. (1) are typically small (<0.3 kcal mol^{-1}) and can be neglected in light of much larger errors associated with some of the other terms.

Using the EA of cyanobenzyl radical, determined in this work, EA(CHPhCN) = 1.90 ± 0.01 eV, the known acidity for the benzyl-α site of benzyl nitrile, $\Delta_{acid}H_{298}$(PhCH$_2$CN) = 1467 ± 9.6 kJ mol^{-1} [21,22], we calculate the BDE corresponding to the formation of the cyanobenzyl radical from benzyl nitrile: DH_{298}(H—CHPhCN) = 80.9 ± 2.3 kcal mol^{-1}. Applying the same procedure to the experimentally determined upper limit of 1.12 eV for the EA of chlorobenzyl radical, and the benzyl-α site acidity of benzyl chloride, $\Delta_{acid}H_{298}$(PhCH$_2$Cl) = 1556 ± 8.8 kJ mol^{-1} [21,23], we determine the upper limit of the BDE of PhCH$_2$Cl, corresponding to the formation of chlorobenzyl radical, DH_{298}(H—CHPhCl) ≤ 84.2 kcal mol^{-1}.

Both of these values represent relatively low BDEs, even more so than our recent determinations for chloro- and fluoro-acetonitriles. To put these values in a context, the BDEs of several related species are summarized in Table 3. For the ease of comparison, the radical stabilization energy (RSE) of each species has been calculated as the corresponding BDE relative to that of methane: RSE(R—H) = DH_{298}(CH$_3$—H) − DH_{298}(R—H). A greater RSE value indicates a weaker R—H bond and a more stable radical R.

Among the mono-substituted methanes listed in Table 3, toluene (PhCH$_3$) has the largest RSE = 15.1 ± 0.5 kcal mol^{-1} [10]. This indicates that among Ph, Cl, and CN, phenyl is the most stabilizing substituent, which may be responsible for most of the RSE magnitudes for α-chloro- and α-cyano-toluenes (PhCH$_2$Cl and PhCH$_2$CN, respectively), determined in the present study.

In general, the RSE action of a substituent may be attributed to effects within the σ and π electron systems of the closed-shell parent molecule and the corresponding radical. As a σ withdrawing group, phenyl ranks low compared to Cl or CN. For this reason, although it stabilizes the closed-shell parent molecule more than the corresponding radical [9], the effect of the σ withdrawing ability of Ph on the parent molecule's BDE is limited. The large RSE effect of Ph is attributed mainly to its π system, which acts as a net π electron acceptor in the extended molecule. This is consistent with the changes observed in acidity for conjugated acids with phenyl substituents [24].

Insight into the strong stabilization observed for the radicals derived from PhCH$_2$CN and PhCH$_2$Cl is offered by the comparison of the RSEs of the chloro- and cyano-substituted species. For homogenously substituted systems with only π-donating or only

π-accepting substituents, the effect of multiple substitutions tend to saturate, i.e. it is typically not additive. For example, the RSE of doubly substituted species tends to be less than the sum of the RSEs of the corresponding mono-substitutions. As seen in Table 3, the RSE of CH$_2$(CN)$_2$ is less than twice that of CH$_3$CN. Similarly, the RSE effect of the third Cl substituent in CHCl$_3$ is small compared to the effects of the first or second substitutions.

In contrast, some heterogeneously substituted systems do not exhibit similar saturation. For them, the RSE was found to be additive or even more than additive. That is, the overall RSE effect of a heterogeneous double substitution (e.g., CN and Cl) is similar or greater than the sum of the CN and Cl mono-substituted RSEs [8,9]. This was specifically observed in species combining the π donating and π accepting groups and was therefore interpreted as a captodative effect of the substituents.

In relation to the present work, the upper bound of the RSE determined for PhCH$_2$Cl is slightly greater than the sum of the CH$_3$Ph and CH$_3$Cl values. We conclude that the effect of the heterogeneous Ph and Cl substitution is at least additive, consistent with the captodative interaction of the π accepting and π donating substituents (Ph and Cl, respectively). Conversely, the RSE of CH$_2$PhCN is 1.8 kcal mol^{-1} less than the sum of the corresponding CH$_3$Ph and CH$_3$CN values (Table 3). Within the same conceptual framework, this result is consistent with both substituent groups in PhCH$_2$CN being π acceptors (hence, no captodative effect).

5. Summary

We have reported the EA for the cyanobenzyl radical, EA(PhCHCN) = 1.90 ± 0.01 eV, and assigned the upper limit of EA for the chlorobenzyl radical, EA(PhCHCl) ≤ 1.12 eV. These results were used to determine the BDEs of the corresponding closed-shell parent molecules through the gas-phase acidity/electron affinity thermodynamic cycle. The C—H BDE of benzyl nitrile at the benzyl-α site was found to be: DH_{298}(H—CHPhCN) = 80.9 ± 2.3 kcal mol^{-1}, while the corresponding BDE of benzyl chloride was assigned an upper bound of DH_{298}(H—CHPhCl) ≤ 84.2 kcal mol^{-1}. These determinations fall in line with the previous studies of homogeneously substituted radicals, which exhibit saturation of the substituent effects on the RSE, and the more recent studies of heterogeneously substituted species, which sometimes display a synergistic (captodative) interaction of π donating and π accepting substituents.

Appendix A. Supplementary data

Supplementary data associated with this article can be found, in the online version, at doi:10.1016/j.cplett.2014.09.001.

References

[1] G. da Silva, E.E. Moore, J.W. Bozzelli, J. Phys. Chem. A 113 (2009) 10264.
[2] J.E. Hodgkins, E.D. Megarity, J. Am. Chem. Soc. 87 (1965) 5322.
[3] F. Bernardi, N.D. Epiotis, W. Cherry, H.B. Schlegel, M.H. Whangbo, S. Wolfe, J. Am. Chem. Soc. 98 (1976) 469.
[4] A.S. Menon, D.J. Henry, T. Bally, L. Radom, Org. Biomol. Chem. 9 (2011) 3636.
[5] S.J. Blanksby, G.B. Ellison, Acc. Chem. Res. 36 (2003) 255.
[6] CRC Handbook of Chemistry and Physics, CRC Press, Boca Raton, FL, 2014–2015.
[7] H.G. Viehe, Z. Janousek, R. Merenyi, L. Stella, Acc. Chem. Res. 18 (1985) 148.
[8] D. Khuseynov, A.R. Dixon, D.J. Goebbert, A. Sanov, J. Phys. Chem. A 117 (2013) 10681.
[9] A.R. Dixon, D. Khuseynov, A. Sanov, J. Phys. Chem. A 118 (2014), dx.doi.org/10.1021/jp5024229.

[10] R.F. Gunion, M.K. Gilles, M.L. Polak, W.C. Lineberger, Int. J. Mass Spectrom. 117 (1992) 601.
[11] L. Velarde, T. Habteyes, A. Sanov, J. Chem. Phys. 125 (2006) 114303.
[12] T. Habteyes, L. Velarde, A. Sanov, Chem. Phys. Lett. 424 (2006) 268.
[13] J. Lee, J.J. Grabowski, Chem. Rev. 92 (1992) 1611.
[14] A.T.J.B. Eppink, D.H. Parker, Rev. Sci. Instrum. 68 (1997) 3477.
[15] A.J.R. Heck, D.W. Chandler, Annu. Rev. Phys. Chem. 46 (1995) 335.
[16] V. Dribinski, A. Ossadtchi, V.A. Mandelshtam, H. Reisler, Rev. Sci. Instrum. 73 (2002) 2634.
[17] D.M. Neumark, K.R. Lykke, T. Andersen, W.C. Lineberger, Phys. Rev. A 32 (1985) 1890.
[18] S.J. Cavanagh, S.T. Gibson, M.N. Gale, C.J. Dedman, E.H. Roberts, B.R. Lewis, Phys. Rev. A 76 (2007) 052708.
[19] M.J. Frisch, et al., Gaussian 09, Gaussian Inc., Wallingford, CT, 2009.
[20] G.D. Dahlke, S.R. Kass, Int. J. Mass Spectrom. 117 (1992) 633.
[21] P.J. Linstrom, in: W.G. Mallard (Ed.), NIST Chemistry WebBook, NIST Standard Reference Database No. 69, National Institute of Standards and Technology, Gaitnersburg, MD, 2013 http://webbook.nist.gov/chemistry/
[22] M. Fujio, R.T. Mciver, R.W. Taft, J. Am. Chem. Soc. 103 (1981) 4017.
[23] J.C. Poutsma, J.J. Nash, J.A. Paulino, R.R. Squires, J. Am. Chem. Soc. 119 (1997) 4686.
[24] J.E. Bartmess, J.A. Scott, R.T. McIver, J. Am. Chem. Soc. 101 (1979) 6056.
[25] J.E. Bartmess, J.A. Scott, R.T. McIver, J. Am. Chem. Soc. 101 (1979) 6046.
[26] S. Moran, H.B. Ellis, D.J. Defrees, A.D. Mclean, G.B. Ellison, J. Am. Chem. Soc. 109 (1987) 5996.
[27] D.J. Goebbert, L. Velarde, D. Khuseynov, A. Sanov, J. Phys. Chem. Lett. 1 (2010) 792.